Single-Column Sub-Grid Cumulus Model for the Atmospheric Radiation Measurement Program

R. B. Stull
University of Wisconsin
Madison, WI 53706

Heterogeneous Surface Forcings

Variations in surface albedo, moisture, soil type, vegetation coverage, and other factors cause surface-layer air (air within 50 m of surface) to be horizontally heterogeneous over land surfaces. This heterogeneity causes patchiness in boundary layer cloud coverage because clouds are formed in thermals of rising surface-layer air.

For climate models, grid cell dimensions are so large that many of these variations are subgrid scale. However, the effect of these variations can be captured via their statistical distributions within each grid cell, and parameters describing these distributions can be used to forecast subgrid scale boundary-layer clouds.

Two phases make up this research: calibration and modeling. First, we use high-resolution turbulence data measured by aircraft over heterogeneous regions to determine the nature of the actual distributions as a function of surface characteristics and solar and atmospheric forcings. Second, the resulting distributions are parameterized using similarity theory and applied in simplified form to forecast cloud coverage and cloud characteristics over other surfaces around the world where no aircraft measurements are feasible.

Prior to the Atmospheric Radiation Measurement/Cloud and Radiation Testbed (ARM/CART) sites coming on line, we have been using existing data from the Hydrologic Atmospheric Pilot Experiment (HAPEX) field experiment in southwest France to develop techniques to determine the statistical distributions. These methods are now refined enough to apply to the preliminary ARM/CART data, such as the data gathered by Steve Oncley from the National Center for Atmospheric Research (NCAR) during his calibration flights in the fall of 1992. We understand that Oncley's data will become available during March 1993. Data from other research flights over the ARM/CART sites will be used as they become available.

Calibration of Subgrid Statistics

During the HAPEX experiment, one frequently flown flight track was an S-shaped pattern, shown in Figure 1. The track passed over 12 different regions of land use, which can be grouped into five broad classes. From 8 May through 24 July 1986, the NCAR King Air aircraft flew the

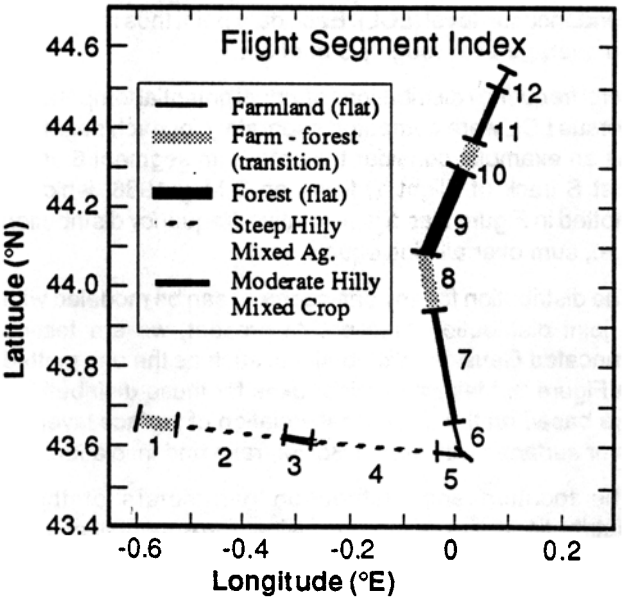

Figure 1. Land usage under HAPEX flight track.

S-track on 21 days, three times a day. Most of these S-tracks were flown at an altitude of 50 to 100 m above ground level.

While the scientists' logs indicated approximate starting and ending times for each flight leg, the aircraft was usually not fully stabilized during portions of the beginning and end of each leg after or prior to turns or changes in altitude. Detailed post-flight data on aircraft pitch, yaw, roll, altitude, heading, and speed have been analyzed to determine flight stability. The erratic portions of the beginning and ends of flight legs were discarded where necessary.

Although the flight legs were flown over fixed visual landmarks, the recorded data contained navigation errors associated with drift in the aircraft inertial-navigation system. Such navigation errors did not accumulate uniformly during any one flight; hence, end-of-flight measurements of location error were inadequate to make corrections to the mid-flight data. Instead, offset errors in latitude and longitude were estimated by eye, separately for each full S-track.

The navigationally corrected portions of stabilized flight observations were then split into segments corresponding to the 12 land-use regions. For each segment, the 20-Hz temperature, pressure, and humidity data were analyzed to compute 20-Hz values of virtual potential temperature, convective available potential energy, and lifting condensation level (LCL). Each data point thus represents an average over roughly 5 m of air.

Joint frequency distributions of virtual potential temperature versus LCL were computed separately for each segment. As an example, consider the data from segment 6 of the first S-track of Flight 1, flown on 9 May 1986, which is plotted in Figure 2 as a joint relative-frequency distribution (i.e., sum over all bins equals one).

The distribution for any one segment can be modeled with a joint distribution function. At present, we are testing truncated Gaussian distributions, such as the one plotted in Figure 3. Major and minor axes for these distributions are based on the theoretical variation of surface layer air over surfaces with varied Bowen ratio and insolation.

The location and distribution parameters of these distributions are analyzed using maximum likelihood methods. Location parameters (mean LCL and mean potential temperature) are then corrected for nonstationarity, because boundary level temperature and humidity evolve with time during the duration of any one flight track.

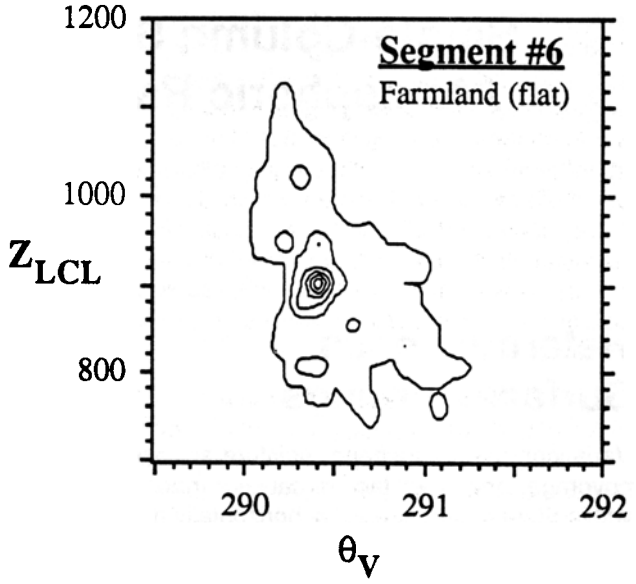

Figure 2. Discrete relative frequency distribution of virtual temperature, θ_v, and height of the lifting condensation level, z_{LCL}, as observed in surface-layer air during segment 6, track 1, flight 1 of HAPEX. Tic marks indicate the sorting bin size. Contours drawn every 0.02, except first contour at 0.001; max. relative freq. = 0.12.

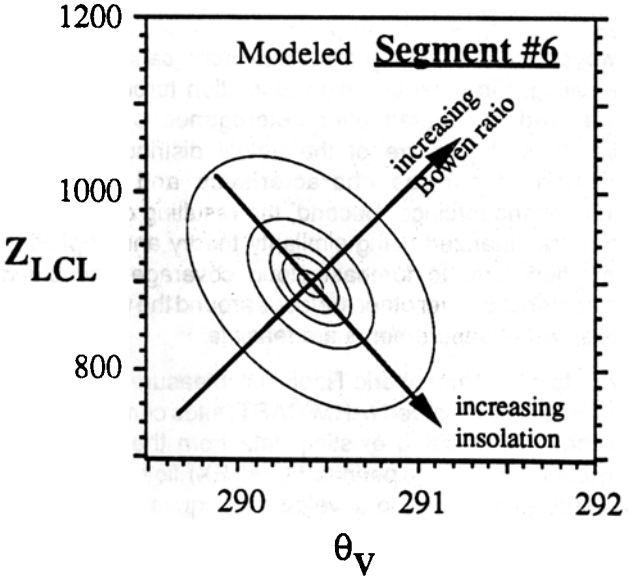

Figure 3. Truncated Gaussian distribution that models the joint distribution data from Figure 2.

The parameters yielding the best-fit distributions are expected to differ from segment to segment. We will normalize these parameters with respect to boundary layer scaling variables to give dimensionless groups. These dimensionless groups will then be organized by broad land-use class. Within any one land-use class, we expect the dimensionless parameters to change gradually during the modeled months as crops mature and are harvested and expect shorter-term variations associated with rain events. If we can observe these changes, we will include them in the parameterization of the distribution functions.

Any single column of a climate model can contain a wide range of land-use regions. A land-use inventory will allow us to construct a modeled joint frequency distribution that is a composite built from weighted sums of the many individual (single-segment) distributions. This is illustrated in Figure 4, where only a few individual distributions are combined to yield a synthetic grid-average distribution.

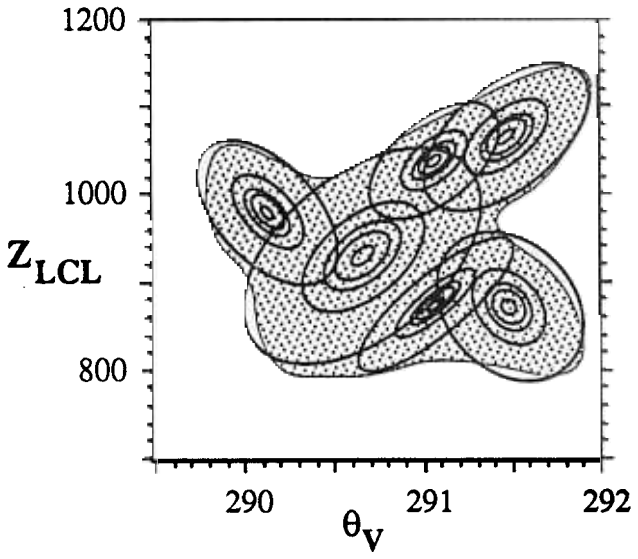

Figure 4. Illustration of a synthetic single-column joint frequency distribution (shaded) of θ_v and z_{LCL}, formed as a composite of many simpler (Figure 3 type) distributions.

Phenomenological Processes

Only the portion of surface-layer air that is positively buoyant will rise as convective thermals. Most of this air remains undiluted during its rise to the top of the mixed layer. Such a thermal is a physical phenomenon with known characteristics that can be employed in a cloud model.

Each thermal has a buoyancy based on its surface-layer virtual potential temperature, and thus will rise to a final equilibrium height that depends on the environmental sounding. Also, each thermal will have a computable lifting condensation level, based on its surface-layer temperature and humidity.

If the height of a thermal is greater than its lifting condensation level, then it will form a cloud. The fraction of area covered by thermals that reach their LCL equals the fractional cloud coverage.

This process can be graphically represented by plotting the joint frequency distribution of surface-layer virtual potential temperature versus z_{LCL} (see above), and superimposing on it a graph of environmental sounding virtual potential temperature versus z. For example, a point within the frequency distribution that is to the right of the sounding represents those air parcels with z_{LCL} lower than the top of the thermal, assuming that an air parcel will conserve its virtual potential temperature as it rises until it hits the sounding. This is demonstrated in Figure 5.

In other words, the integral over that portion of the frequency distribution that is to the right of the sounding gives the fraction of sky covered by clouds, assuming that the distribution was previously normalized such that an integral over the whole function equals one.

Forecast Model

To implement this scheme in a single column of a climate model, one must forecast the evolution of both the environmental sounding of Figure 5 and the location of the frequency distribution. The former is easy using a simple slab model of the mixed layer. Such a model forecasts the vertically unresolved mixed-layer top, z_i, and average mixed-layer temperature θ_{ML} and humidity q_{ML}. The latter is easily forecast by using bulk-transfer relationships to estimate the amount of excess temperature and humidity in the surface layer compared with the mixed layer.

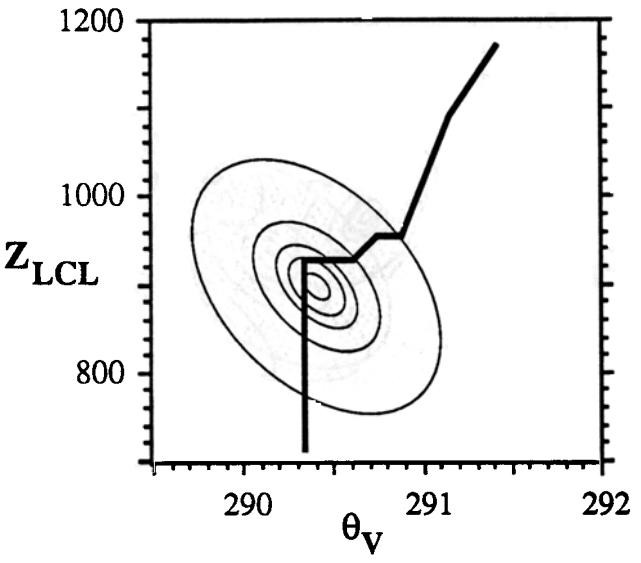

Figure 5. Contours represent values of constant frequency distribution of virtual potential temperature θ_v versus z_{LCL} for surface-layer air. Superimposed is a plot of the environmental sounding of θ_v versus height z.

Temperature and humidity, $\theta(z)$ and $q(z)$, are known (resolved) in a single-column model in the early morning. This provides data for the initial sounding. Imposed on the boundary layer are surface values of kinematic heat H and moisture E fluxes. Let the mean surface layer (SL) conditions give the location for the frequency distribution. The forecast equations are

$$w_e = 0.2 \cdot H / [\theta(z_i) - \theta_{ML}]$$

$$dz_i / dt = w_e$$

$$d\theta_{ML} / dt = 1.2 \cdot H / z_i$$

$$dq_{ML} / dt = \{E - w_e \cdot [q(z_i) - q_{ML}]\} / z_i$$

$$\omega^* = \{(g/\theta_{ML}) \cdot z_i \cdot [H \cdot (1 + 0.61\, q_{ML}) + 0.61 \cdot \theta_{ML} \cdot E]\}^{1/3}$$

$$\theta_{SL} = \theta_{ML} + H/(0.0063 \cdot w^*)$$

$$q_{SL} + q_{ML} + E/(0.0063 \cdot w^*)$$

As illustration, consider an initial state similar to Figure 5, except that the whole frequency distribution is completely above the sounding. Namely, the surface layer is sufficiently dry that the lifting condensation levels for all surface-layer air parcels are well above the top of the early morning mixed layer. Thus, there would be no clouds. Later in the day as the mixed layer grows and the LCL distribution moves, a portion of the distribution might be below the sounding, giving a nonzero cloud-cover forecast.

This procedure, except using the composite distribution as in Figure 4, will be used in the single-column model to make the cloud cover forecasts for forced clouds. Separate equations would be added to model the transformation of forced clouds into active and passive ones. The total boundary-layer cloud cover is the sum of these dynamic cloud types.

Summary

The approach reported here uses subgrid statistics together with phenomenological characteristics of thermals to produce a diagnosis of cloud cover and other characteristics. Hence the name "stochastic-phenomenological" parameterization. When this parameterization is combined with a forecast model of the boundary layer, the result is a computationally efficient yet physically realistic parameterization for subgrid boundary-layer clouds within any single column of a climate-model.